# A Novel Strain Stiffening Model for Magnetorheological Elastomer Base Isolator and Parameter Estimation Using Improved Particle Swarm Optimization

Yang Yu, Yancheng Li and Jianchun Li*

*Abstract*—**In order to fully utilize the advantages of magnetorheological elastomer (MRE) base isolator for seismic protection of civil structures, a high fidelity model should be established to characterize its nonlinear hysteresis for its implementation in structural control. In this paper, a novel strain stiffening model is developed to capture this unique characteristic. In this model, a strain stiffening component, which described the unique viscos-elastic behavior of the device, is incorporated with a Voigt element, which portrays the solid-material behavior. The new model, as an attractive feature, maintains a relationship between the isolator parameters and physical force-displacement nonlinear phenomenon and decreases the complexity in other existing models. In addition to the proposed model, an improved optimization algorithm based on particle swarm optimization (IPSO) is designed to identify the model parameters by utilizing experimental force-displacement-velocity data acquired from various loading conditions. In this new algorithm, the mutation operation in genetic algorithm is utilized for helping the model solution avoiding the local optimum. The superiority of the proposed model and parameter solving algorithm is validated by comparing them with the classical Bouc-Wen model and other optimization algorithms through the error analysis, respectively. The comparison results show that the proposed model can exactly predict the force-displacement and force-velocity responses at both small and large displacements, and has a smaller root-mean-square (MSE) error than the Bouc-Wen model. Compared with other optimization algorithm, the IPSO not only has a faster convergence rate, but also obtains the satisfactory parameters identification results.**

## I. Introduction

Seismic protection of civil structures plays a major role in rescuing resources and lives. Base isolation, as the most popular seismic protection technique, has been widely applied to buildings and bridges as a result of its great superiority during the earthquakes. The principle of the isolation system is to incorporate additional base isolators between the foundation and the protected structures. In accordance with the acceleration design response spectra, the acceleration response is able to remarkably decline with the decrease of the fundamental frequency. Though the deformation may be raised, it is mainly focused on the base isolator and few deformations are generated in the isolated structures [1, 2].

So far, a variety of base isolation systems have been designed, such as tuned mass damper roller pendulum, lead rubber bearing, sand cushion, etc [3]. They have been utilized in the buildings all over the world. Although some of them have withstood the seismic test and exhibited the good performance, the main deficiency in existing base isolation systems is that one isolation system, which is good for one type of earthquake, may be out of work during another type of earthquake. Related studies have shown that due to their passive nature, most existing isolation systems are especially vulnerable to two kinds of earthquakes, i.e. the near-fault and far-fault earthquakes [4].

To deal with this problem, various solutions have been presented, including supplementary damping hybrid and other hybrid isolation systems [4]. However, these systems have their own benefits and drawbacks. Some limitation still exists when they are applied into practice. Recently, with the development of the intelligent material, the semi-active vibration isolation based on magnetorheological elastomer (MRE) are studied to enhance the traditional devices in vibration control of structures [5-7]. Opie et al. designed a MRE based vibration isolator with alterable stiffness, which descends resonances and payload velocities by 16% and 30%, respectively [8]. Du et al. developed a smart isolator using the variable stiffness performance of MRE and applied to the vehicle seat suspension system [9]. Kavlicoglu et al. devised a new MRE mount with two-layer MREs to provide a wide controllable compression static stiffness [10]. For the development of adaptive base isolation system of civil structures, Behrooz et al. proposed a novel MRE vibration isolation system with tunable natural frequency by adjusting the amplitude of acceleration input under different applied currents [2]. Li et al. successfully designed first full-scale base isolator utilizing 45 layers of MREs with stiffness increase around 38% [11]. Li et al. devised another adaptive MRE seismic isolator with 25 soft MRE laminated layers which achieved significant adjustable range of horizontal stiffness, i.e. more than 16 folds

*Corresponding author.

Jianchun Li is with the University of Technology Sydney, Sydney, NSW 2007 Australia (corresponding author to provide phone: +61-2-9514 2651; fax: +61-2-9514 2633; e-mail: jianchun.li@uts.edu.au).

Yang Yu is with the University of Technology Sydney, Sydney, NSW 2007 Australia (e-mail: yang.yu@uts.edu.au).

Yancheng Li is with the University of Technology Sydney, Sydney, NSW 2007 Australia (e-mail: yancheng.li@uts.edu.au).

[4, 12]. The MRE base isolator proposed by Li et al [4, 11-12] is the first device with laminated rubber layers which is likely to be accepted for engineering application.

Although the MRE isolator is favorable in the field of vibration control, the main challenge for its engineering application rests on the nonlinear force-displacement/velocity responses. Generally, to design a controller with a traceable model is challenging when the MRE isolator is employed. However, the research on modeling for MRE devices is relatively less. Chen et al. designed a linear rheological model to forecast the performance of MRE working under various magnetic fields, strain amplitudes and frequencies [13]. Yang et al. explored the field-dependent stiffness/damping characteristics of MRE base isolators proposed by Li et al. and developed a Bouc-Wen based model to reproduce its unique dynamic behaviors [14]. Behrooz et al. presented a phenomenological model consisted of springs, viscous damping and a Bouc-Wen element to capture the behavior of the MRE isolator with variable stiffness and damping [2]. The models mentioned above vary from the simplest visco-elastic model to complicated models with differential equations. However, it is worth nothing that all MRE models show a tradeoff between the model accuracy and computational demand. As a result of a large number of parameters required and multiple nonlinear differential equations, the identification of the model parameters is complicated and difficult to implement. Particle swarm optimization (PSO), as a swarm intelligent method, has been developed for processing the complicated problems, which are difficult to be solved by other approaches [15]. PSO has been successfully applied to several fields, such as model identification. However, due to the randomness of the algorithm parameters, the standard PSO always has a slow convergence rate and is apt to trap into the local optimum.

In this study, a novel hysteresis model for MRE base isolator is presented. The new model adopts a strain stiffening module together with the traditional viscous damping and spring stiffness to stand for the unique hysteretic behavior of the MRE base isolator. Then, a type of improved PSO is designed to aiming at the differential equations in the proposed model. In this new algorithm, a mutation operator is introduced to the standard PSO for avoiding the model solution from the local optimum. The improvement is able to guarantee a faster convergence rate in the identification process and the higher recognition accuracy for identification results.

The outline of the paper is given as follows. Several existing MRE models for describing the MRE behaviors are illustrated in the next section. Section III gives the proposed model together with the statement of the optimization problem for parameter identification. In section IV, the improved PSO, applied to estimate the model parameters, is exploited and its advantages are emphasized. Parameter identification results and algorithm performance are discussed in Section V. Eventually, Section VI draws the conclusion.

## II. Existing Hysteresis Models

### A. Bouc-Wen Model

The Bouc-Wen model is the widest applicable model for hysteresis modeling. This model consists of a Bouc-Wen operator, symbolizing the hysteretic characteristic, combined with the traditional damping and stiffness components, standing for the solid material behavior. The Bouc-Wen model is usually represented by a damping force combined with a hysteresis variable, given as [14]:

$$\begin{aligned} F &= \alpha k_0 x + (1-\alpha) k_0 z + c_0 \dot{x} \\ \dot{z} &= A\dot{x} - \beta |\dot{x}| |z|^{n-1} z - \gamma \dot{x} |z|^n \end{aligned} \tag{1}$$

where $\alpha$, $A$, $\beta$, $\gamma$ and $n$ are non-dimensional parameters which are used to adjust the shape and scale of the hysteretic loops; $k_0$ and $c_0$ denote the spring stiffness and damping viscosity coefficients; $z$ is an intermediate variable to signify the time-series function of the displacements. The Bouc-Wen model is widely used in structure engineering and MR behavior because of its numerical capacity to demonstrate all sorts of hysteresis. However, because of the incorporation of internal dynamics in regard to the hysteretic variable $z$, undesirable singularities may appear in the process of model parameter identification.

### B. Improved Dahl Model

Yu et al. suggested a simple and effective improved Dahl model for MRE base isolator [16]. In this model, instead of the Bouc-Wen operator, a Dahl hysteretic component is incorporated for reconstructing the Coulomb force to prevent the identification of excessive parameters. The improve Dahl model is capable of well portraying the hysteretic force-displacement response in the small displacement region and can be expressed as:

$$\begin{aligned} F &= k_0 x + c_0 \dot{x} + \delta z - f_0 \\ \dot{z} &= \rho(\dot{x} - |\dot{x}| z) \end{aligned} \tag{2}$$

where $\delta$ is a parameter for the shape of the force-displacement response, $f_0$ denotes the initial bias force and $\sigma$ denotes the stiffness coefficient. The improved Dahl model can be regarded as a particular case of the general Bouc-Wen model, which has fewer parameters.

### C. Hyperbolic Hysteresis Model

Regardless of the Bouc-Wen or Dahl models, the expressions of the differential equation increase the model complexity, which makes the model difficult to be identified. Concerning this issue, a hyperbolic hysteresis model is designed, which includes a hysteresis component, denoted by a hyperbolic sine function, combined with the viscous damper and spring stiffness [17]. The expression of the hyperbolic hysteresis model is given as:

$$F = c_0\dot{x} + k_0 x + \gamma \sinh(\alpha x) + f_0 \tag{3}$$

where $\gamma$ and $\alpha$ denote the scale factors of the hysteresis and slope, respectively. Compared with other models, the hyperbolic hysteresis model is liable to be identified by conventional searching methods with high recognition accuracy. However, this model is not able to clarify the Mullins effect in the MRE base isolator.

## III. Proposed Model and Problem Statement

### A. The Proposed Model

Against the disadvantages in existing models, this paper puts forward a novel strain stiffening model to forecast the nonlinear behaviors of the MRE base isolator, shown in Fig. 1. The new model consists of a three-parameter solid model as well as an improved Maxwell model, which has a strain stiffening component and a dashpot element connected in series. The new dashpot element $c_1$ is to introduce variable transition to strain stiffening behavior for the MRE base isolator. The new model can be expressed by:

$$\begin{aligned} F &= k_1 y + \alpha z^3 \\ k_1 y &= k_0 (x - y) + c_0 (\dot{x} - \dot{y}) \\ \alpha z^3 &= c_1 (\dot{x} - \dot{z}) \end{aligned} \tag{4}$$

where $c_0$, $k_0$, $c_1$, $k_1$ and $\alpha$ denote the model parameters to be identified, and $y$ and $z$ are intermediate dynamical variables.

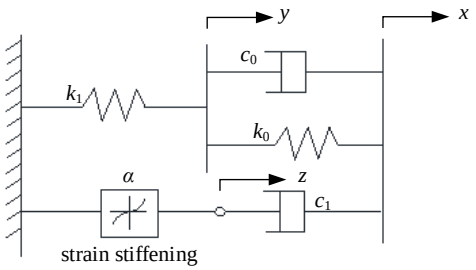


Figure 1. The proposed strain stiffening model.

### B. Problem Statement

Compared with the Bouc-Wen model, the new proposed model has less model parameters for identification. Due to the differential equations in the model, model parameters are not easy to be searched by attempts. Thus a minimization optimization is adopted to deal with the model solution. The critical factor for solving an optimization problem is to construct a reasonable fitness function, which is of great importance to the identification result. Here, the Euler formula is used to solve the differential equations in the model and the fitness function is defined as follows:

$$\begin{aligned} H(X) &= \frac{1}{N}\sum_{i=1}^{N}[F_i - (k_1 y_i + \alpha z_i^3)]^2 \\ y_{i+1} &= y_i + \Delta t \cdot [-\frac{(k_0 + k_1)}{c_0} \cdot y_i + \dot{x}_i + \frac{k_0}{c_0} \cdot x] \\ z_{i+1} &= z_i + \Delta t \cdot [-\frac{\alpha}{c_1} \cdot z_i^3 + \dot{x}_i] \end{aligned} \tag{5}$$

where $F_i$, $x_i$ and $\dot{x}_i$ denote the force, displacement and velocity at time $t_i$, respectively; $\Delta t$ is the sampling time interval; $N$ represents the total number of the experimental data. If the fitness value approximates to zero, identification result $X$=[$\alpha$, $c_0$, $k_0$,

$c_1$, $k_1$] is regarded as the optimal solution. As a consequence, this optimization problem is able to be described with some constraints:

$$\begin{aligned}
&\min_X H(X) = \frac{1}{N}\sum_{i=1}^{N}[F_i - (k_1 y_i + \alpha z_i^3)]^2 \\
&y_{i+1} = y_i + \Delta t \cdot [-\frac{(k_0 + k_1)}{c_0} \cdot y_i + \dot{x}_i + \frac{k_0}{c_0} \cdot x] \\
&z_{i+1} = z_i + \Delta t \cdot [-\frac{\alpha}{c_1} \cdot z_i^3 + \dot{x}_i] \\
&s.t.\ k_0 > 0,\ c_0 > 0,\ k_1 > 0,\ c_1 > 0,\ y(0) = 0,\ z(0) = 0
\end{aligned} \tag{6}$$

## IV. METHODOLOGY

### A. Particle Swarm Optimization

The principle of PSO is described as: the animal swarm is made up of *P* particles. Every particle is related to its position $x_i$ and velocity $v_i$. Initially, the positions and velocities of all the particles are randomly assigned by the vectors in the restricted scales. Then, the particles are assessed on the basis of values of the objective function of optimization problem. By comparing these function values, every particle stores itself optimal position as $pbest_i$ as well as the global optimal position as *gbest*. The searching process of standard PSO is expressed as [18]:

$$\begin{cases} v_i^{k+1} = w_i v_i^k + c_1 rand_1(pbest_i - x_i^k) + c_2 rand_2(gbest - x_i^k) \\ x_i^{k+1} = x_i^k + v_i^{k+1} \end{cases} \tag{7}$$

where *w* denotes the inertia weight factor; $c_1$ and $c_2$ denote the acceleration coefficients, represented by two constants; $rand_1$ and $rand_2$ denote random numbers between 0 and 1. In this paper, a linearly declining inertia weight factor employed, which is defined as:

$$w = w_{\max} - \frac{(w_{\max} - w_{\min})}{N_{iter}} n \tag{8}$$

where *n* and $N_{iter}$ denote the current and maximal iteration number, respectively; $w_{max}$ and $w_{min}$ denote two boundaries of inertia weight factor.

### B. Improved Particle Swarm Optimization

Although PSO algorithm has been widely applied to model parameter estimation, the prematurity convergence problem still exists in the identification process especially when the identified model is too complicated. Due to two differential equations in the proposed model, the standard PSO may be ineffective for parameter identification unless the good initial values are selected. Therefore, an improved PSO (IPSO) is designed to avoid excessive local search for the prematurity convergence.

In the improved algorithm, the mutation operation is introduced after updating the particle position to prevent the algorithm from the local optimum. Especially, the global optimal solution may remain unchanged with the increase of the iteration number in the later stage of search. For this problem, a mutation factor in genetic algorithm is incorporated into standard PSO to avoid the particle trapping into the local optimal value. If the global optimum still keeps the same after a number of iteration, a slight disturbance is incorporated into the velocity of a randomly selected particle by a pre-set mutation rate $p_m$. Here, $p_m$ is set according to the maximal velocity of the particle. Thus the velocity of the particle *i* in dimension *d* is updated by:

$$v_{id}^{k+1} = \begin{cases} v_{id}^{k+1} + sign(rand_3 - 0.5) \cdot rand_3 \cdot v_{\max}, & if\ rand_3 < p_m \\ v_{id}^{k+1}, & or\ else \end{cases} \tag{9}$$

where $rand_3$ is a random number between 0 and 1 and $p_m$ denotes the mutation rate. The mutation rate could enable a random particle to get out of the swarm, and make it flight across the solution domain which is not searched previously. This improvement can enhance the search ability of the swarm to explore the global optimal value. Moreover, when the mutation condition is satisfied, the divergent problem will not appear because the swarm has recorded the global optimum as *gbest*.

### C. Process of Parameter Identification with IPSO

The identification process by IPSO consists of the following steps, shown in Fig. 2.

*Step 1.* Confirm the optimization problem to be solved and initialize the algorithm parameters: the optimization problem has been defined in previous section (Model Section). The IPSO algorithm parameters include the particle population size $P$, the maximal allowable velocity $v_{max}$, acceleration coefficients $c_1$ and $c_2$, boundaries of inertia weight factor $w_{max}$ and $w_{min}$, the mutation rate $p_m$, the maximal iteration number $N_{iter}$ and so on.

*Step 2.* Randomly assign the position and velocity vectors of each particle by the following equation:

$$\begin{aligned} x_{id} &= x_{dl} + rand \cdot (x_{du} - x_{dl}) \\ v_i &= rand \cdot v_{\max} \end{aligned} \tag{10}$$

*Step 3.* Calculate the value of fitness function of each particle. Evaluate and record the individual optimal position and global optimal position by the following equation:

$$pbest_i^{k+1} = \begin{cases} pbest_i^k, & if\ f(x_i^{k+1}) \geq f(pbest_i^k); \\ x_i^{k+1}, & or\ else \end{cases} \tag{11}$$

*Step 4.* Update the position and velocity of each particle according to (8) and (7).

*Step 5.* Calculate the value of fitness function of each particle.

*Step 7.* If the fitness $f(gbest)$ is unchanged after $N_{mu}$ iterations, the mutation operation starts: a particle from the swarm is randomly chosen and its velocity is update according to (9). Or else, go to *Step 8*.

*Step 8.* Check the termination rule. There are several rules available to stop the PSO algorithm according to the problem domain. Here, the maximal iteration is employed as the termination condition, in which $N_{iter}$ is set to a fixed constant. Moreover, if the maximal iteration number is satisfied, calculation is terminated and *gbest* is stored as the best solution. Or else, *Step 3* is repeated.

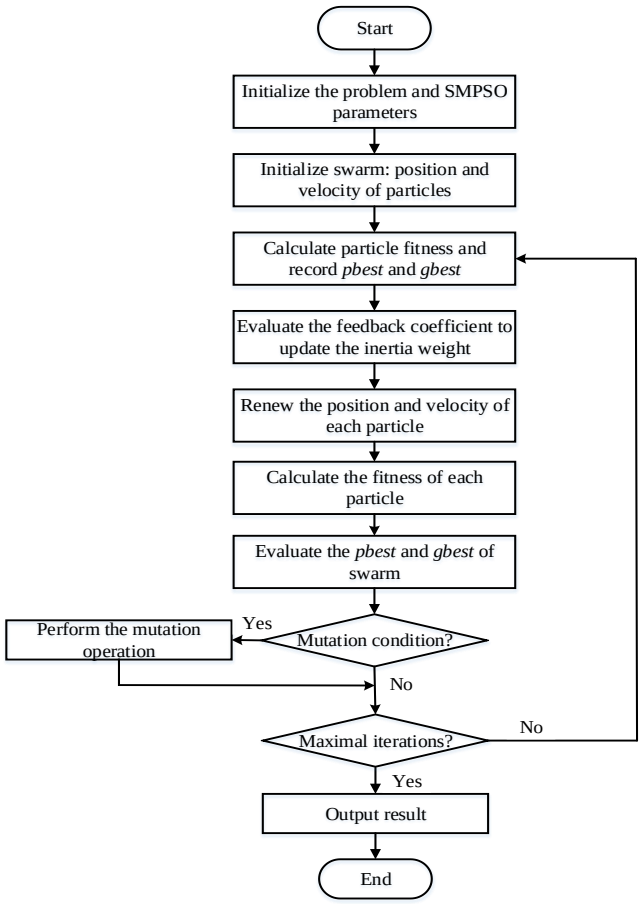


Figure 2. Algorithm process for parameter identification.

## V. IDENTIFICATION RESULTS AND DISCUSSION

### A. Experimental Setup

A sequence of experimental tests are carried out to measure the responses of a MRE base isolator, which are fed into the improved PSO to estimate the parameters of the proposed strain stiffening model. In every experiment, the device is excited with a sinusoidal signal with different displacement amplitudes, excitation frequencies and supplying currents. The displacements vary from 2mm to 8mm, the excitation frequencies are between 0.1Hz and 4Hz, and the supplying currents range from 0A to 3A. The total of 48 groups of experimental data is concluded, shown in Table I. Moreover, the identification is conducted using the proposed model and the Bouc-Wen model by the improved PSO. The algorithm parameters are set as: $P$=60, $c_1$=$c_2$=1.4962, $w_{max}$=0.9, $w_{min}$=0.2, $N_{iter}$=400, $N_{mu}$=10, $p_m$=0.6 and $v_{max}$=2.

TABLE I. EXPERIMENTAL CONDITIONS

| **Current (A)** | **Frequency (Hz)** | | | |
|---|---|---|---|---|
| | ***0.1*** | ***1*** | ***2*** | ***4*** |
| 0 | 2/4/8 mm | 2/4/8 mm | 2/4/8 mm | 2/4/8 mm |
| 1 | 2/4/8 mm | 2/4/8 mm | 2/4/8 mm | 2/4/8 mm |
| 2 | 2/4/8 mm | 2/4/8 mm | 2/4/8 mm | 2/4/8 mm |
| 3 | 2/4/8 mm | 2/4/8 mm | 2/4/8 mm | 2/4/8 mm |

### B. Model Identification Results

In order to evaluate the capacity of the proposed strain stiffening model to predict the nonlinear responses of the MRE base isolator, a group of parameters are identified for the model to fit the experimental data (4Hz-frequency, 4mm-displacement and 3A-current). Fig. 3 shows the tracking process in one sampling period and the relative errors between the experimental and reconstructed data, respectively. It is clearly seen that the relative errors are kept between -7% and 7%, which is allowable in the modeling. Fig. 4 (a) depicts the hysteretic relationship between force and displacement while Fig. 4 (b) demonstrates the nonlinear force-velocity response. It is obvious that the reconstructed force perfectly matches the experimental data.

To further assess the effectiveness of the proposed model for describing the hysteretic and nonlinear behaviors of the MRE base isolator, more groups of identification results are compared between experimental and reconstructed data in different loading conditions. Fig. 5 shows the displacement-force and velocity-force responses of the MRE base isolator loaded with three different amplitudes (2mm, 4mm and 8mm) sinusoidal at the frequency of 4Hz and the current of 3A. It is noted that the proposed model yields good agreements with the experimental data.

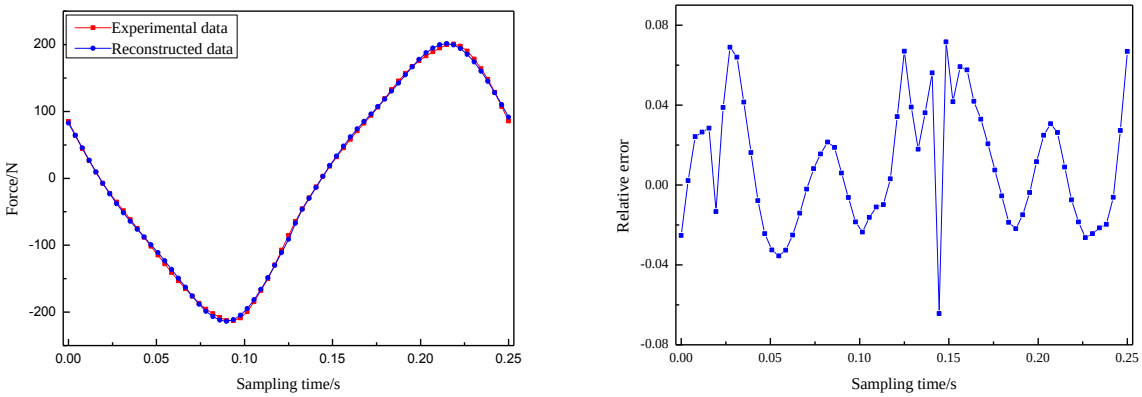


(a) Tracking process (b) Relative errors

Figure 3. Algorithm process for parameter identification.

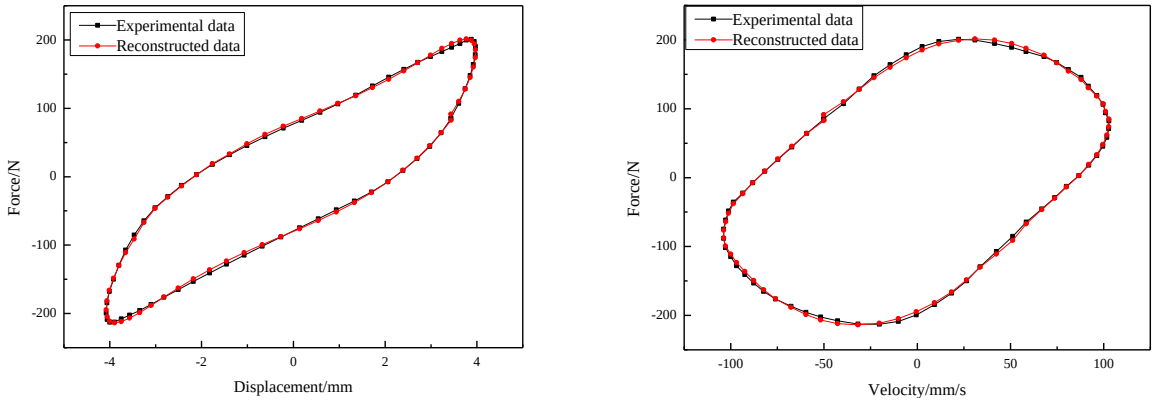


(a) Force-displacement responses (b) Force-velocity responses

Figure 4. Comparison between experimental and reconstructed data.

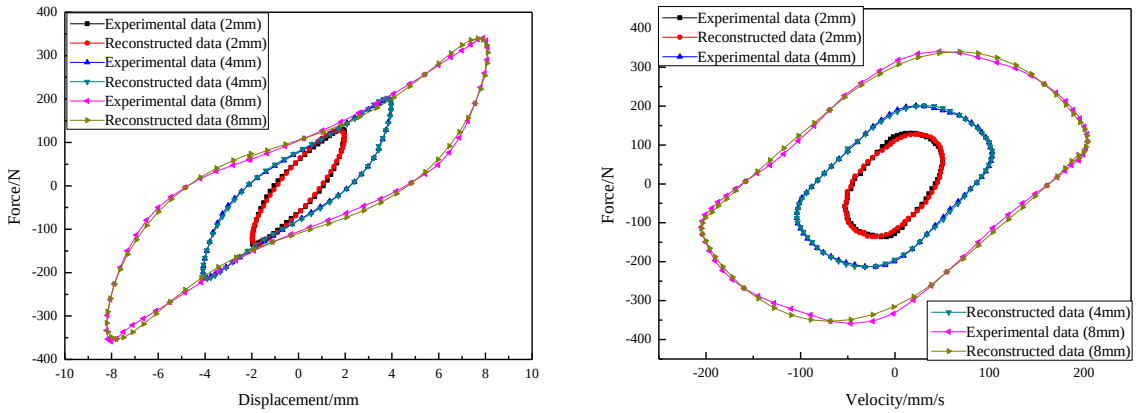


(a) Force-displacement responses (b) Force-velocity responses

Figure 5. Evaluation responses of the proposed model in different amplitudes.

Fig. 6 illustrates the influence of the varying frequency on the property of the MRE base isolator. From Fig. 6, it is obvious that the excitation frequency has a light effect on the maximal force and effective stiffness. Especially, in the condition of the frequency above 0.1Hz, the testing force and effective stiffness stay almost unchanged with the increasing frequency. Unlike the force-displacement relationship, the increasing frequency leads to the ascending nonlinearity of the force-velocity relationship.

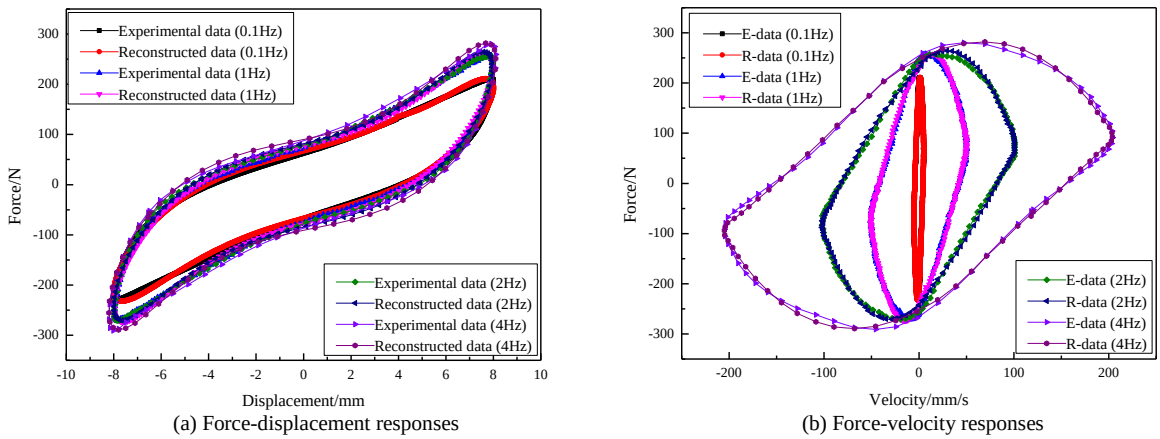


(a) Force-displacement responses (b) Force-velocity responses

Figure 6. Evaluation responses of the proposed model in different excitation frequencies.

The predicted displacement-force and velocity-force pairs displayed in Fig. 7 are gained by supplying the device with 4mm amplitude and 4Hz frequency sinusoidal at four different currents (0A, 1A, 2A and 3A). The comparison results indicate the forecasting capacity of the strain stiffening model to describe the ascending hysteretic and nonlinear responses with the increasing supplied currents. Moreover, when the current maintains as a constant, the reconstructed loops of the proposed model are perfectly matched with the experimental data of the MRE base isolator.

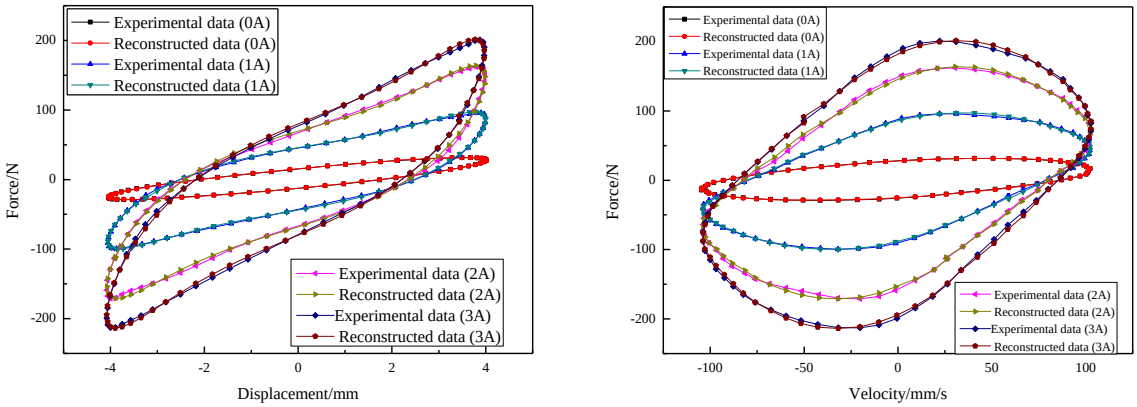


(a) Force-displacement responses (b) Force-velocity responses

Figure 7. Evaluation responses of the proposed model in different applied currents.

## C. *Modeling Error Analysis*

In order to test the accuracy of the proposed model, a quantitative study is carried out to appraise the mean square error (MSE) between the experimental and reconstructed data. Here, the MSE is defined as:

$$e_{mse} = \frac{1}{N_v}\sum_{i=1}^{N_v}[F_{rec}(i) - F_{\exp}(i)]^2 \tag{12}$$

where $F_{rec}$ and $F_{exp}$ denote the reconstructed and experimental data of the MRE base isolator, respectively; $i$ is the $i$th data set in the data array; $N$ is the length of the data array. Additionally, the Bouc-Wen model is adopted to compare with the proposed one for model error analysis. Fig. 8 shows the comparison results in the cases of 1Hz and 4Hz. It is obviously seen that as a result of the higher degree nonlinearity in the Bouc-Wen model, the bigger MSE errors are shown from the reconstructed force from the model.

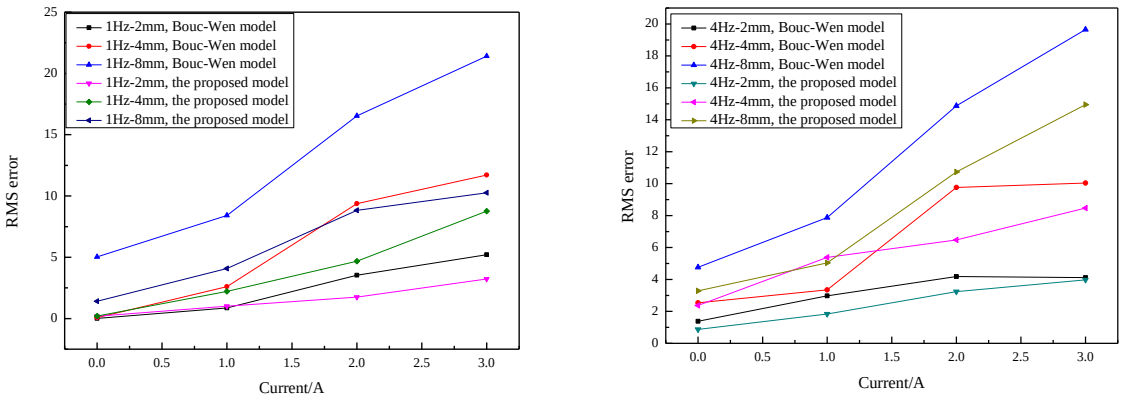


(a) 1Hz excitation frequency (b) 4Hz excitation frequency

Figure 8. MSE errors for both the proposed and Bouc-Wen models.

## D. *Algorithm Performance Discussion*

In the improved PSO algorithm, the mutation operator $p_m$ is regarded as a new parameter to prevent the result from the local optimum. Therefore, the influence of $p_m$ on the algorithm performance is studied in this part. Fig. 9 describes the

convergence of the MAFSA with different mutation operators over 400 iterations under the loading condition of 1A current, 1Hz sinusoid and 4mm amplitude. Here, several methods are utilized to set a pm. The direct method is to define its value as a constant. In this part, five cases of constant $p_m$ are selected (0, 0.2, 0.4, 0.6 and 0.8). Another method is to define as a linearly decreasing function in the range of 1 and 0. This method enables a higher $p_m$ to be adopted for the mutation operation in the initial phase of the identification process. With the process of the identification, a comparatively lower $p_m$ will be adopted. It can be seen from Fig. 9 that the mutation of 0 results in the premature convergence. Moreover, it is clearly seen that the mutation rate of 0.6 outperfoMSE others, which is regarded as the optimal choice.

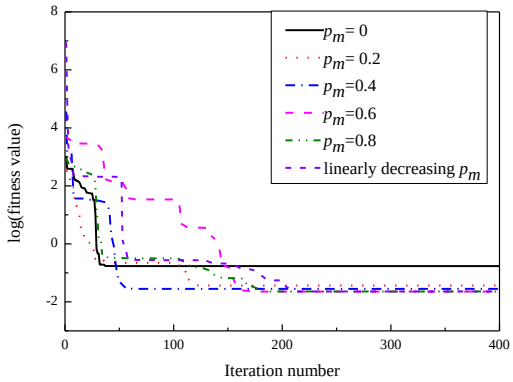


Figure 9. Convergence comparison for IPSO with different mutation operators.

To demonstrate the superiority of the adaptive weight in the IPSO algorithm, two other optimization algorithms are utilized for performance comparison: standard PSO and genetic algorithm (GA) [16]. For the purpose of impartial evaluation, the standard PSO is set the same parameter values as the IPSO. Fig. 10 illustrates the final results by comparing the convergence rate. Despite the fact that the standard PSO has the fast rate among four algorithms, it leads to the premature convergence. Unlike the standard PSO, the IPSO algorithm has the highest identification accuracy and reaches its optimum more quickly than GA.

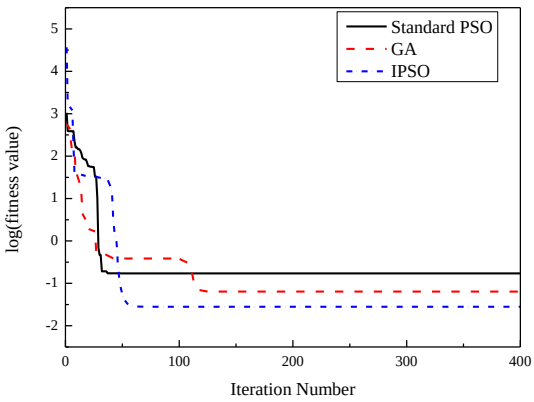


Figure 10. Convergence comparison for different algorithms.

## VI. Conclusion

This paper presents a new string stiffening based model for MRE base isolator to depict the force-displacement hysteretic behavior. This model requires five model parameters, which is less than that of the Bouc-Wen model. An improved optimization algorithm based on PSO is presented for model parameter identification. Concerning the issue that the algorithm has a slow searching rate in the later stage of the identification process, a mutation operation is employed to prevent the algorithm falling into the local optimum. Testing data from a practical MRE base isolator are utilized for modeling verification. The results indicate that the novel model is capable of modeling the MRE base isolator and the designed IPSO algorithm is effective for model parameter identification.

## References

[1] G. Jia and Z. Shi, "A new seismic isolation system and its feasibility study," *Earthq. Eng. Eng. Vib.*, vol. 9, no. 1, pp. 75-83, Mar. 2010.

[2] M. Behrooz, X. Wang and F. Gordaninejad, "Modelling of a new semi-active/passive magnetorheological elastomer isolator," *Smart Mater. Struct.*, vol. 22, no. 4, article no. 045013, Apr. 2014.
[3] F. Yao, S. Shang and K. Liu, "Shake table tests of a new steel-asphalt composite layer system for the seismic base isolation of housing units," *Soil Dyn. Earthq. Eng.*, vol. 59, pp. 1-7, Feb. 2014.
[4] C. P. Providakis, "Effect of supplemental damping on LRB and FPS seismic isolators under near-fault ground motions," *Soil. Dyn. Earthq. Eng.*, vol. 29, no. 1, pp. 80-90, Jan. 2009.
[5] Y. Li, J. Li, T. Tian and W. Li, "A highly adjustable magnetorheological elastomer base isolator for applications of real-time adaptive control," *Smart Mater. Struct.*, vol. 22, no. 9, article no. 095020, Sep. 2013.
[6] M. Yalcintas and H. Dai, "Vibration suppression capabilities of magnetorheological materials based adaptive structures," *Smart Mater. Struct.*, vol. 13, no. 1, article no.1, Feb. 2004.
[7] N. Hoang, N. Zhang and H. Du, "A dynamic absorber with a soft magnetorheological elastomer for powertrain vibration suppression," *Smart Mater. Struct.*, vol. 18, no. 7, article no. 074009, Jul. 2009.
[8] S. Opie and W. Yim, "Design and control of a real-time variable stiffness vibration isolator," in *Proc. of Advanced Intelligent Machatronics*, Singapore, 2009, pp. 380-385.
[9] H. Du, W. Li and N. Zhang, "Semi-active variable stiffness vibration control of vehicle seat suspension using an MR elastomer isolator," *Smart Mater. Struct.*, vol. 20, no. 10, article no. 105003, Jul. 2011.
[10] B. Kavlicoglu, B. Wallis, H. Sahin and Y. Liu, "Magnetorheological elastomer mount for shock and vibration isolation," in *Proc. of Active and Passive Smart Structures and Integrated Systems*, San Diego, 2011, article no. 79770Y.
[11] Y. Li, J. Li, W. Li and B. Samali, "Development and characterization of a magnetorheological elastomer based adaptive seismic isolator," *Smart Mater. Struct.*, vol. 22, no. 3, article no. 035005, Mar. 2013.
[12] J. Li, Y. Li, W. Li and B. Samali, "Development of adaptive seismic isolators for ultimate seismic protection of civil structures," in *Proc. of Sensors and Smart Structures Technologies for Civil, Mechanical, and Aerospace Systems*, San Diego, 2013, article no. 86920H.
[13] L. Chen and S. Jerrams, "A rheological model of the dynamic behaviour of magnetorheological elastomers," *J. Appl. Phys.*, vol. 110, no .1, article no. 013513, Jul. 2011.
[14] J. Yang, H. Du, W. Li, Y. Li, J. Li, S. Sun and H. X. Deng, "Experimental study and modeling of a novel magnetorheological elastomer isolator," *Smart Mater. Struct.*, vol. 22 , no.117001, Nov. 2013.
[15] N. M. Kwok, Q. P. Ha, T. H. Nguyen, J. Li and B. Samali, "A novel hysteretic model for magnetorheological fluid dampers and parameter identification using particle swarm optimization," *Sens. Actuators A: Phys.*, vol. 132, no. 2, pp. 441-451, Nov. 2006.
[16] Y. Yu, Y. Li and J. Li, "Parameter identification of an improved Dahl model for magnetorheological elastomer base isolator based on enhanced genetic algorithm," In *Proc. of 23rd Australasian Conference on the Mechanics of Structures and Materials*, Baron Bay, 2014, accepted.
[17] Y. Yu, Y. Li and J. Li, "Parameter identification of a new hysteretic model for magnetorheological elastomer base isolator using modified artificial fish swarm algorithm," *In Proc. of International Symposium on Automation and Robotics in Construction and Mining*, Sydney, 2014, accepted.
[18] I. Trelea, "The particle swarm optimization algorithm: convergence analysis and parameter selection," *Inf. Process. Lett.*, vol. 85, no. 6, pp. 317-325, Mar. 2003.